Evidence for a 3.45-billion-year-old magnetic remanence: Hints of an ancient geodynamo from conglomerates of South Africa

著者	Usui Yoichi, Tarduno John A., Watkeys Michael, Hofmann Axel, Cottrell Rory D.
著者別表示	臼井 洋一
journal or publication title	Geochemistry, Geophysics, Geosystems
volume	10
number	9
page range	Q09Z07
year	2009-09-24
URL	http://doi.org/10.24517/00067005

doi: 10.1029/2009GC002496

Geochemistry Geophysics Geosystems G3
AN ELECTRONIC JOURNAL OF THE EARTH SCIENCES
Published by AGU and the Geochemical Society

Article
Volume 10, Number 9
24 September 2009
Q09Z07, doi:10.1029/2009GC002496
ISSN: 1525-2027

Evidence for a 3.45-billion-year-old magnetic remanence: Hints of an ancient geodynamo from conglomerates of South Africa

Yoichi Usui
Department of Earth and Environmental Sciences, University of Rochester, Rochester, New York 14627, USA

Also at Department of Earth Sciences, Tohoku University, Sendai 980-8578, Japan

John A. Tarduno
Department of Earth and Environmental Sciences, University of Rochester, Rochester, New York 14627, USA (john@earth.rochester.edu)

Also at Department of Physics and Astronomy, University of Rochester, Rochester, New York 14627, USA

Michael Watkeys and Axel Hofmann
School of Geological Sciences, University of KwaZulu-Natal, Durban 4000, South Africa

Rory D. Cottrell
Department of Earth and Environmental Sciences, University of Rochester, Rochester, New York 14627, USA

[1] Paleomagnetic and rock magnetic analyses of ~3445-million-year-old dacite conglomerate clasts and parent body rocks from the Barberton greenstone belt, South Africa, define two dominant components of magnetization. One component, unblocked at low temperature, is an overprint acquired ~180 million years ago. The other component is unblocked at high temperatures and passes a conglomerate test, indicating that this component is older than the depositional age of the conglomerate (~3416 Ma). The high unblocking temperature component shows scatter in the parent body rocks that can be explained by the effects of modern lightning strikes, Archean overprinting, and the presence of multidomain magnetic grains that are conducive to carrying secondary magnetizations. Alternatively, this scatter can be explained by exotic magnetization scenarios in the absence of a dynamo, including magnetization by an external field related to solar wind interaction with the atmosphere. Such exotic mechanisms can be tested with the acquisition of paleointensity data. While more scattered than paleomagnetic data recording the more recent geomagnetic field, the high unblocking temperature component in the dacite parent body shows some consistency, and the simplest explanation of the data is that they reflect a geodynamo ~3445 million years ago.

Components: 8940 words, 7 figures, 5 tables.

Keywords: geodynamo; Archean; paleointensity.

Index Terms: 1510 Geomagnetism and Paleomagnetism: Dynamo: theories and simulations; 1521 Geomagnetism and Paleomagnetism: Paleointensity.

Received 12 March 2009; **Revised** 22 June 2009; **Accepted** 30 June 2009; **Published** 24 September 2009.

Usui, Y., J. A. Tarduno, M. Watkeys, A. Hofmann, and R. D. Cottrell (2009), Evidence for a 3.45-billion-year-old magnetic remanence: Hints of an ancient geodynamo from conglomerates of South Africa, *Geochem. Geophys. Geosyst.*, *10*, Q09Z07, doi:10.1029/2009GC002496.

Theme: Magnetism From Atomic to Planetary Scales: Physical Principles and Interdisciplinary Applications in Geoscience
Guest Editors: J. Feinberg, F. Florindo, B. Moskowitz, and A. P. Roberts

1. Introduction

[2] Establishing the early history of the geomagnetic field can provide valuable information about the evolution of the deep interior as Earth cooled. Analyses of lunar nitrogen and noble gases suggest that Earth may have lacked a magnetic field at ~3900 Ma [*Ozima et al.*, 2005]. A thermal model for the cooling of an Hadean-Archean magma ocean suggests the start of the geodynamo between 3900 and 3400 Ma [*Labrosse et al.*, 2007]. Testing for magnetizations of these ages in rocks is hampered by metamorphic overprints and magnetic mineral alteration.

[3] To obtain a pristine paleomagnetic record of the Archean geomagnetic field one must examine rocks with precise age control. One must also carefully consider the potential impact of younger geologic events. In particular, low-grade metamorphism with peak heating temperatures of ~300°C has affected even the best preserved Archean samples. This imposes a series of requirements that need to be met before one can consider a magnetization a primary recording of an ancient geodynamo [*Tarduno et al.*, 2007]. Rock magnetic theory [*Néel*, 1955] calls for the presence of single-domain carriers, and the magnetic mineralogy should be such that blocking temperatures are high (e.g., the Ti content in titanomagnetites should be low). Metamorphism should not have formed new magnetic minerals, which would acquire a younger remanence. In effect, this means the samples should have minimal amounts of reactive iron. Iron-rich Archean materials such as komatiite, basalt and mafic minerals from felsic rocks can contain abundant secondary magnetic minerals and magnetizations.

[4] One way to address these challenges is to examine the magnetization of single-silicate crystals that can host near single-domain magnetite inclusions rather than using whole rock samples [*Cottrell and Tarduno*, 1999; *Smirnov et al.*, 2003; *Tarduno et al.*, 2006]. The tiny size of the magnetic particles, their protection from chemical alteration by the silicate jacket, and the minimal iron contents of the host grains lead to the prediction that single-silicate crystals are the materials most likely to preserve Archean age magnetizations. Samples of quartz and feldspar from plutonic rocks of the Barberton area of southern Africa have yielded data suggesting that Earth's magnetic field strength at 3200 Ma was similar to (at least 50% of) that of the modern field [*Tarduno et al.*, 2007]. This is currently the oldest demonstrable paleomagnetic record of a thermoremanent magnetization (TRM) in terrestrial rocks.

[5] A complement to the single-crystal approach is the use of paleomagnetic field tests that provide direct evidence of the relative age of magnetizations. Here, we conduct a paleomagnetic conglomerate test [*Graham*, 1949] on ~3445-million-year-old rocks from the Kaapvaal Craton to determine whether a magnetic field was present at that time. We will return to the complexities of interpreting magnetizations from bulk rock samples that contain multidomain magnetic grains when we compare results of the conglomerate test to data from the conglomerate parent body.

2. Geology of the Study Area and Paleomagnetic Sampling of the Conglomerate

[6] Pebbles to cobbles of dacite (5–15 cm in size; mean size of ~8 cm) were collected from conglomerates of the Hooggenoeg Formation (Onverwacht Group) in the western part of the Barberton greenstone belt, South Africa (Figure 1). The conglomerate also contains minor clasts of altered mafic/ultramafic rock and chert. The Onverwacht Group consists of a >10 km thick succession of komatiitic and tholeiitic volcanic rocks with minor sedimentary and felsic volcanic units [*Lowe and Byerly*, 1999; *South African Committee for Stra-*

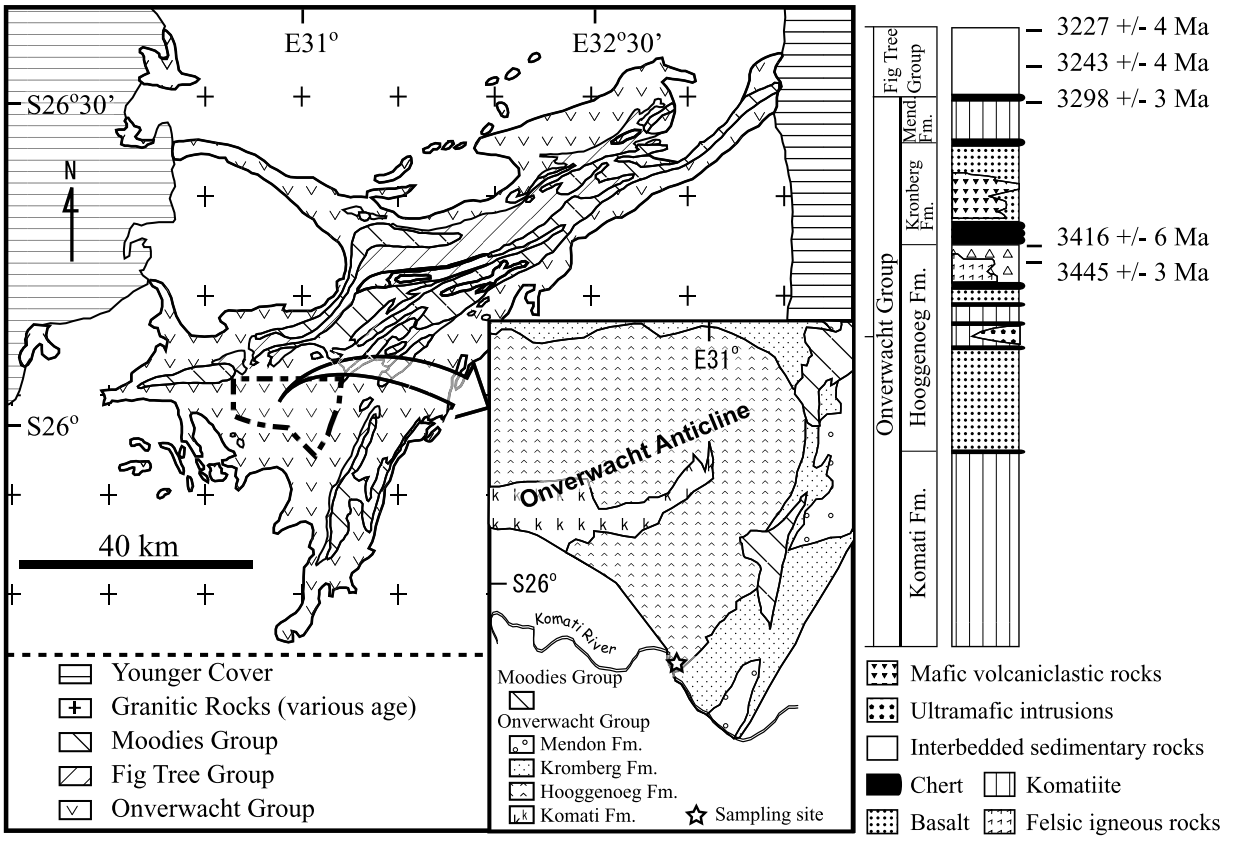

Figure 1. Simplified geological map and stratigraphy of the western Barberton greenstone belt with sampling site. Modified after *Lowe and Byerly* [1999]. Ages in the stratigraphic column are after *Kröner et al.* [1991] and *Byerly et al.* [1996].

tigraphy, 1980; *Viljoen and Viljoen*, 1969]. The uppermost member of the Hooggenoeg Formation consists of massive dacitic intrusive rocks cut by mafic and ultramafic intrusive bodies. The dacite-clast conglomerates sampled in this study locally cover the dacitic intrusion, together with volcaniclastic breccia and sandstone [*Lowe and Byerly*, 1999].

[7] Zircon ages for these dacitic volcanic and volcaniclastic rocks have been reported as 3438 ± 12 Ma [*Kröner and Todt*, 1988], 3445 ± 8 Ma [*Armstrong et al.*, 1990], 3445 ± 3 Ma [*Kröner et al.*, 1991] and 3451 ± 5 Ma [*de Vries et al.*, 2006]. These ages overlap the ages of tonalite-trondhjemite-granodiorite (TTG) plutons surrounding the southern part of the Barberton Greenstone Belt, supporting the interpretation that the Hooggenoeg dacitic rocks and TTG suite are comagmatic [*de Wit et al.*, 1987; *Kröner et al.*, 1991]. A thin tuff from the uppermost part of the dacite-derived siliciclastic unit in the Hooggenoeg Formation was dated as 3416 ± 5 Ma, suggesting the unit including the conglomerate beds was deposited between ~3445 and ~3416 Ma [*Kröner et al.*, 1991].

[8] The central part of the Barberton greenstone belt has suffered regional greenschist facies metamorphism [*Viljoen and Viljoen*, 1969]. Several estimates of peak heating temperature have been reported: ~200°C at ~2700 Ma in the Fig Tree Group based on isotopic resetting in barites [*de Ronde et al.*, 1991] or carbonates [*Toulkeridis et al.*, 1998], and 300 to 400°C for the upper Onverwacht Group and the Fig Tree Group from the degree of graphitization of carbonaceous material in cherts [*Tice et al.*, 2004]. *Cloete* [1999] reported a temperature of 320 ± 25°C for Hooggenoeg Formation pillow basalts stratigraphically below our sampling site on the basis of a fluid inclusion study of interpillow quartz veins. *Xie et al.* [1997] reported a metamorphic temperature of ~320°C from the Onverwacht and Fig Tree Group near the sampling site in this study on the basis of an empirical chlorite geothermometer [*Cathelineau*, 1988]. In summary, the likely peak temperature

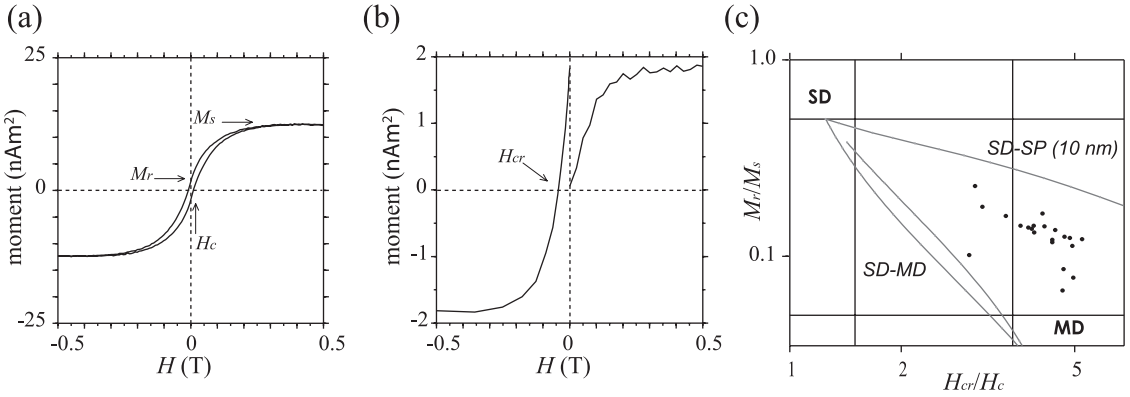

Figure 2. Examples of rock magnetic measurements. (a) A hysteresis curve corrected for paramagnetic slope with the determination of M_r, M_s, and H_c. M_{rs}/M_s is lower than the value for SD magnetite of 0.5. The curve shows slightly constricted shape. (b) Acquisition curve of isothermal remanence and backfield curve with the definition of H_{cr}. (c) Summary of the rock magnetic measurements of 21 samples on a Day plot with theoretical mixing curves for SD-SP and SD-MD mixtures of *Dunlop* [2002]. The results deviate from SD-MD mixing curve toward SD-SP mixing curve.

experienced by our samples is equal to or less than ~350°C.

[9] Oriented dacite hand samples were collected at a well-exposed rock pavement along the Komati River (26°1′S, 30°59′E). We restricted sampling of the conglomerate to hand samples to minimize impact at the locality, which is used for geologic training and general public education. A prominent, large block of conglomerate was avoided because it was found to be out of place. The sampling site is located in a deep river valley, minimizing the risk of lightning strikes on the samples. Sample orientations were measured using a magnetic compass and corrected for local declination. The rocks have a weak NRM intensity and no significant deflection of a magnetic compass during sampling due to the magnetization of rocks was observed (or expected). Three conglomerate horizons separated by sandstones were sampled. The clasts are well rounded and milky white to dark gray in color.

[10] The microscopic texture of the dacite clasts is microcrystalline plagioclase and quartz with some phenocrysts of plagioclase (1–2 mm) and quartz (~0.5 mm). Accessory minerals include magnetite and apatite. The plagioclase phenocrysts are largely replaced by clay minerals.

3. Rock Magnetism of the Conglomerate Clasts

[11] To characterize the magnetic domain state and magnetic stability of the samples, magnetic hysteresis measurements were performed using a Princeton Measurements Alternating Gradient Force Magnetometer (AGFM). The parameters of magnetic hysteresis (M_{rs}, saturation remanence; M_s, saturation magnetization; H_c, coercivity; and H_{cr}, coercivity of remanence) were determined. A Day plot [*Day et al.*, 1977; *Dunlop*, 2002] was constructed, to supply information about the domain state of magnetic phases. Microscopic observation and X-ray microprobe analysis were performed on polished thin sections by a reflected light microscope and a SEM (Zeiss Leo-DSM 982) with a Phoenix EDAX. Low-temperature magnetic behaviors were investigated using a Quantum Design magnetic Property Measurements System (MPMS-XL5) at the Geological Survey of Japan. An isothermal remanent magnetization of 2.5 T was given at 6 K after having cooled down in a zero field. Thermal demagnetization up to 300 K was monitored.

[12] An example of a hysteresis loop and the Day plot is shown in Figure 2a. The M_{rs}/M_s values were lower than theoretical value for single-domain (SD) magnetite grains of 0.5 [e.g., *Dunlop*, 2002], indicating the predominance of multidomain (MD) grains. The hysteresis loops have constricted middles, commonly known as wasp-waisted. On the Day plot, the results fall above the theoretical mixing line of MD grains with SD grains [*Dunlop*, 2002] (Figure 2c). These observations suggest the presence of very small grains in the superparamagnetic (SP) range and/or the presence of magnetic minerals with distinctly different coercivities [*Dunlop*, 2002; *Jackson et*

al., 1993; *Tarduno and Myers*, 1994; *Tauxe et al.*, 1996].

[13] Thin-section observations reveal the presence of magnetite (Figure 3) which exhibit internal reflections along irregular cracks. This suggests the early stages of partial low-temperature oxidation [*Johnson and Hall*, 1978; *Petersen and Vali*, 1987]. X-ray microprobe analysis detected Fe but no Ti in the magnetite. Low-temperature isothermal remanent magnetization (Figure 4) indicates the presence of the Verwey transition of magnetite [*Verwey*, 1939]. This result also suggests that the oxidation is very minor ($z < 0.3$, where z is the oxidation parameter of *O'Reilly and Banerjee* [1967]) [*Özdemir et al.*, 1993]. We conclude that very slightly oxidized magnetite, varying in domain state from SP to MD, is the dominant magnetic carrier in our samples. We cannot exclude, however, the minor presence of other oxides, such as goethite and hematite, which are common weathering products that might also be expected in these surface samples.

4. Paleomagnetism of the Conglomerate Clasts

[14] Standard paleomagnetic cores or cubes were prepared from each hand sample using nonmagnetic diamond drill bits and saws. Progressive thermal demagnetization was employed for magnetic cleaning and was carried out in an ASC Scientific TD-48 thermal demagnetizer. The magnetization of the samples was measured using a 2G DC SQUID magnetometer with high-resolution sensing coils. The thermal demagnetizer and magnetometer are located in a magnetically shielded room in the University of Rochester. Magnetic directions of individual samples were determined utilizing principal component analysis technique [*Kirschvink*, 1980]. Mean directions were computed with *Fisher* [1953] statistics.

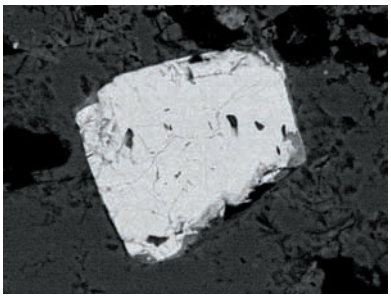

Figure 3. Backscattered electron image showing irregular shrinkage crack in magnetite grain from sample KR1-2.

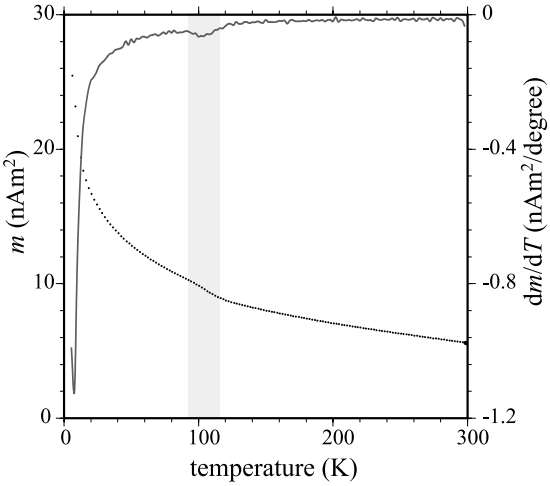

Figure 4. Thermal demagnetization of a 2.5 T isothermal remanent magnetization acquired at 6 K showing a steepening of slope at ~110 K due to the Verwey transition of magnetite. Gray line is the derivative of the demagnetization data.

[15] During thermal demagnetization, low-temperature components were removed by ~500°C to ~560°C (Figure 5). The low-temperature components usually consisted of multiple components; however there was sometimes one prominent direction. We will call this direction the low unblocking component or LT (Figures 5a and 5b). The LT magnetizations group around a common in situ direction (D = 338.4°, I = −60.3°, α_{95} = 6.5, k = 45.5 (Table 1)). The LT direction is similar to that from the ~180 Ma Karoo basalts [*Hargraves et al.*, 1997]; Karoo age overprints have been observed in Neoarchean basalts from other parts of the Kaapvaal Craton [*Strik et al.*, 2007]. However, The LT direction is also close to the present-day geomagnetic field at the site (Figure 6a). We thus interpret the LT magnetization as a thermoviscous overprint, acquired at, or younger than 180 Ma.

[16] At unblocking temperatures above ~500°C to ~560°C, a characteristic high-temperature component (HT) was isolated from 24 samples taken from 14 clasts (Table 2). The other samples exhibit continuous changes in remanence direction during demagnetization (Figure 5c) preventing isolation of remanence components. This behavior is typical of thermal overprints carried by MD grains [e.g., *Dunlop and Özdemir*, 1997]. The break in unblocking temperature between the LT and HT components (i.e., ~500°C to ~560°C) is much higher

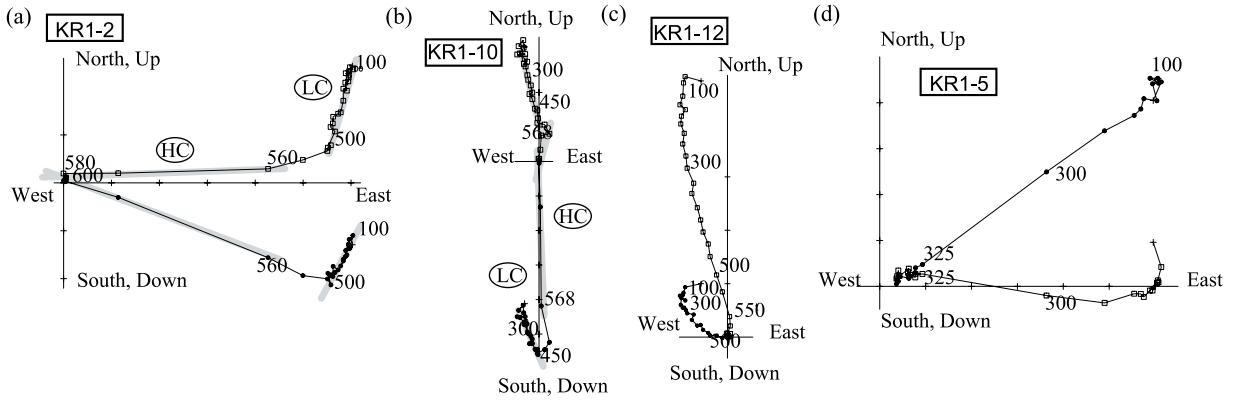

Figure 5. Orthogonal vector plots of thermal demagnetization result for representative samples. Heating steps are indicated in °C. The results for (a) KR1-2 and (b) KR1-10 reveal both low unblocking temperature (LT) and high unblocking temperature (HT) magnetizations (see section 4). (c) The result for KR1-12 shows continuous curvature suggesting the strong contribution from MD grains. (d) Sample KR1-5 shows nearly complete unblocking by demagnetization temperatures of ∼350°C (see section 4 for discussion of potential magnetic carriers in this anomalous sample).

than the highest peak metamorphic temperature (i.e., ∼350°C). This can be explained as partial thermoremanence "tails" of MD grains [*Dunlop and Özdemir*, 1997]. The natural remanent magnetization of the samples unblocked at around 580°C, supporting the rock magnetic conclusion that the magnetic carrier is magnetite with only minor oxidation.

[17] The magnetization of one fine-grained cobble (KR1-5) exhibits an unusually large decay between 300 and 325°C (Figure 5d). SEM analyses reveal Ti oxide grains in specimens from this clast; remanence-carrying grains appear to be less than a few microns in size. Low-temperature data lack the Verwey transition or the magnetic transition characteristic of pyrrhotite, whereas coercivity values are relatively low and atypical of ilmenohematite. Although the exact magnetic carrier in this anomalous clast is uncertain, potential magnetic minerals include maghemite, titanomagnetite and titanomaghemite.

[18] Although two steep directions (KR1-11 and KR1-3) are somewhat close to a ∼2.8 Ga Archean

Table 1. Low-Temperature Component From Dacitic Clasts[a]

Clast	Specimen	Range (°C)	*N*	MAD	*D* (deg)	*I* (deg)	*k*	α_{95}
KR1-2	1	225.0–475.0	11	6.7	21.4	−71.1		
	2	75.0–500.0	18	8.8	9.7	−58.9		
	3	275.0–400.0	6	9.7	336.7	−54.6		
Clast mean					359	−62.8	34	21.3
KR1-3	1	0.0–525.0	21	5.4	351.4	−68.7		
KR1-4	1	100.0–550.0	19	6.2	345	−62		
	2	0.0–250.0	10	5.3	13.5	−60		
Clast mean					359.7	−61.8	68	30.6
KR1-6	1	350.0–500.0	7	4.5	333.8	−57.1		
	2	450.0–525.0	4	5.6	327.1	−57.3		
Clast mean					330.5	−57.2	995	7.9
KR1-10	1	300.0–450.0	7	6.7	319.5	−60.2		
	2	300.0–475.0	8	7.8	317.7	−55.9		
Clast mean					318.5	−58.1	677	9.6
KR1-11	1	225.0–350.0	6	6.5	319.7	−60.9		
	2	300.0–500.0	9	5.3	310.2	−61.1		
Clast mean					315	−61.1	619	10.1
Mean for six clasts					338.4	−60.3	46	6.5

[a] *N*, number of demagnetization steps used; MAD, maximum angular deviation; *D*, declination, *I*, inclination; *k* and α_{95}, *Fisher* [1953] statistical parameters.

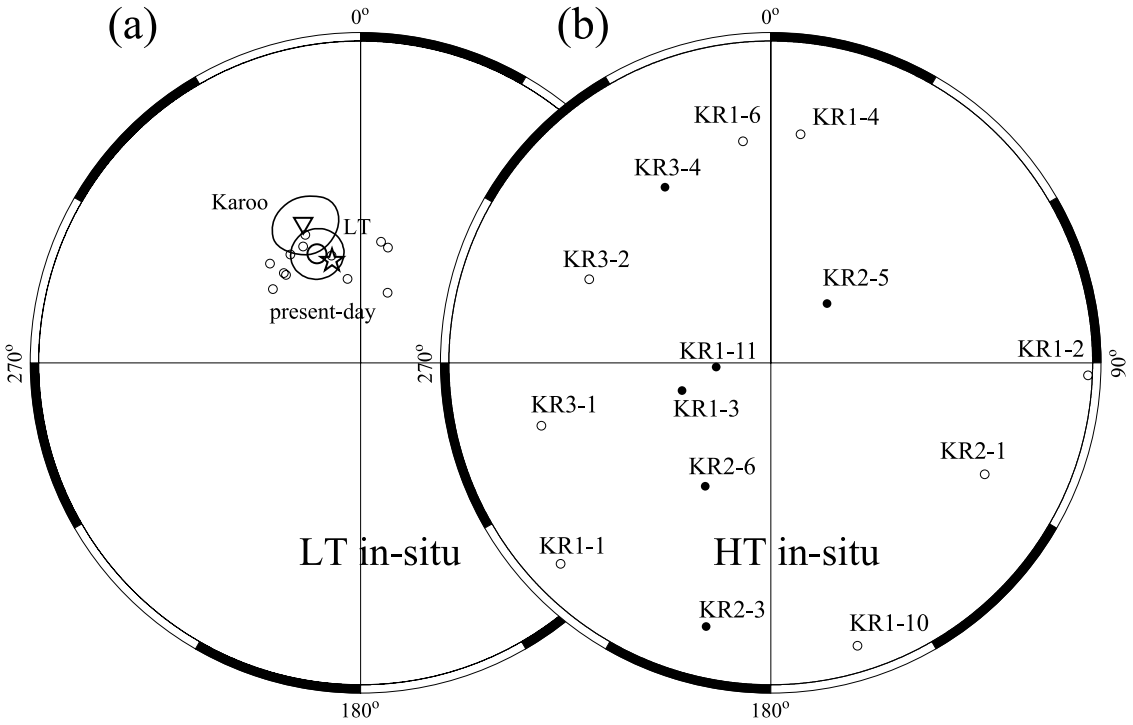

Figure 6. Equal area projections showing paleomagnetic directions. Open symbols are upper hemisphere projection, and filled symbols are lower hemisphere projection. (a) Mean direction for the low unblocking temperature (LT) magnetization (circle) with 95% confidence interval together with magnetic direction from the Karoo basalt (triangle [after *Hargraves et al.*, 1997]) and present-day geomagnetic field (star). Small circles are paleomagnetic directions derived from individual samples. (b) High unblocking temperature (HT) magnetizations from different clasts. Results of individual samples and statistics are given in Table 2.

overprint direction discussed by *Tarduno et al.* [2007], overall the HT directions from the 14 clasts appear to be drawn from a random population (Table 2 and Figure 6b). The randomness of the HT direction was investigated using *Watson*'s [1956] test. The length (R) of the resultant vector of the unit vectors directed along the HT direction was compared with the critical values R_0 calculated from *Fisher* [1953] statistics. These 14 samples revealed $R = 2.37$. This value is smaller than the critical value of $R_0 = 5.98$ at the 95% significance level, suggesting that they are from a statistically random population. This result provides evidence that the HT magnetization of the dacite clasts was acquired before deposition of the conglomerate beds that contains them (~3416 Ma).

[19] Although *Graham* [1949] in his classic study outlining the conglomerate test sampled both a conglomerate and the parent rock, a comparison of the magnetization character of clasts and their source was not proposed as a formal requirement of the test. As an extreme example, conglomerate tests have been reported from meteorites for which the parent rock is not on Earth [e.g., *Weiss et al.*, 2002; *Kirschvink et al.*, 1997]. Nevertheless, it has been implied in many subsequent descriptions of the conglomerate test that knowledge of the parent rock demagnetization characteristics can provide important context [e.g., *McElhinny*, 1973; *Butler*, 1992]. In particular, there is sometimes a concern that if the parent rock is magnetically unstable, its derivative clasts might also be unstable; this lack of magnetic stability might mimic a positive conglomerate test.

[20] The issue of magnetic stability of the parent rock is of special importance for our investigation for several reasons. Unlike other studies of terrestrial samples, where the question to be answered is one of the age of magnetization, we are exploring the absence/presence of a geodynamo at 3445 Ma. Conceivably, the lack of a geodynamo during cooling of the dacite might ultimately result in a highly scattered magnetization pattern (see section 6). In addition, all the dacite samples examined clearly contain some MD magnetic grains, and we expect these to carry overprints acquired during Archean low-grade metamorphism. Therefore, we do not expect the high unblocking temperature

Table 2. High-Temperature Component From Dacitic Clasts[a]

Clast	Specimen	Range (°C)	*N*	MAD	*D* (deg)	*I* (deg)	*k*	α_{95}
KR1-1	1	560.0–580.0+0	3	5.8	226.1	−10.7		
KR1-2	1	550.0–580.0+0	4	2.2	89	0.3		
	2	550.0–580.0+0	4	3.3	91.1	−2.4		
	3	560.0–580.0+0	3	2.6	91.7	−2.4		
	4	550.0–580.0+0	4	3.7	97.5	1.4		
Clast mean					92.3	0.8	387	4.7
KR1-3	1	550.0–580.0+0	4	2.5	272.6	69.6		
	2	550.0–580.0+0	4	3.1	237.2	62.1		
Clast mean					252.2	66.8	51	35.6
KR1-4	1	560.0–580.0+0	3	6.5	5.6	−24.9		
	2	560.0–580.0+0	3	7.5	13.6	−16.3		
	3	525.0–580.0+0	5	3.1	2.8	−45.9		
Clast mean					7.8	−29.1	26	24.8
KR1-6	1	560.0–584.0+0	5	2.5	354.8	−32.8		
	2	560.0–584.0+0	4	1.2	351.4	−30.8		
Clast mean					353.1	−31.8	1064	7.7
KR1-10	1	568.0–584.0+0	3	1.5	160.1	−9.6		
	2	560.0–584.0+0	4	1	165.3	−7.3		
Clast mean					162.7	−8.5	414	12.3
KR1-11	1	550.0–576.0+0	4	1.3	265.4	75.7		
	2	560.0–584.0+0	4	1.7	267.1	77.8		
Clast mean					266.2	76.8	2880	4.7
KR2-1	1	560.0–584.0+0	4	1.1	118.9	−27.0		
	2	560.0–584.0+0	4	0.6	116	−23.9		
Clast mean					117.4	−25.5	798	8.9
KR2-3	1	560.0–580.0+0	3	5.9	193.4	17.1		
KR2-5	1	560.0–580.0+0	3	1.1	44.4	69.1		
KR2-6	1	560.0–580.0+0	3	0.6	207.4	54.4		
KR3-1	1	545.0–580.0+0	4	2.7	254.6	−27.3		
KR3-2	1	560.0–580.0+0	3	4.5	294.9	−38.3		
KR3-4	1	560.0–580.0+0	3	0.4	329.3	36.7		

[a] *N*, number of demagnetization steps used (does not include the origin); MAD, maximum angular deviation; *D*, declination; *I*, inclination; *k* and α_{95}, *Fisher* [1953] statistical parameters. In the temperature range, "+0" indicates the origin was included in the fit.

component to record a pure primary thermoremanent magnetization. Instead, it will at best record a primary TRM contaminated with minor MD overprints that will contribute to the overall directional scatter. To examine these issues, we next move to a study of the dacite parent rocks.

5. Paleomagnetic Study of the Dacite Source Rock

[21] The intrusive dacite parent body is from the same stratigraphic sequence as the conglomerate, and therefore our sampling forms the more rigorous intraformational version of the conglomerate test [e.g., *Butler*, 1992]. We sampled the dacite parent body at 5 sites over an approximately 75 m transect (Figure 7), collected as a series of drilled cores (sites 1–2) and hand samples (sites 1 and 3–5), along a small, remote creek on the Geluk farm in the Barberton greenstone belt (see location map given by *Lowe and Byerly* [1999]). All sites were from a local topographic low, although sites 1–3 were on a more exposed, flat area. Samples were prepared as standard specimens for thermal demagnetization using the same techniques described in our study of the conglomerate clasts.

[22] Thermal demagnetization experiments reveal both consistency and variation in the directional content between sites (Figure 7 and Tables 3–5). Samples from some cores drilled at sites 1 and 2 show a southwesterly positive inclination component unblocked at high temperatures, after the removal of a low unblocking temperature component. (Note that all directions are discussed in geographic coordinates. We make no attempt here to correct these for the complex structural folding of the area). Other samples at these sites, and a hand sample comprising site 3, have a single component of magnetization (Table 3). These single-component magnetizations are variable in direction and probably represent modern lightning strikes. Still other samples were unstable during demagnetization, showing evidence for laboratory-induced alteration

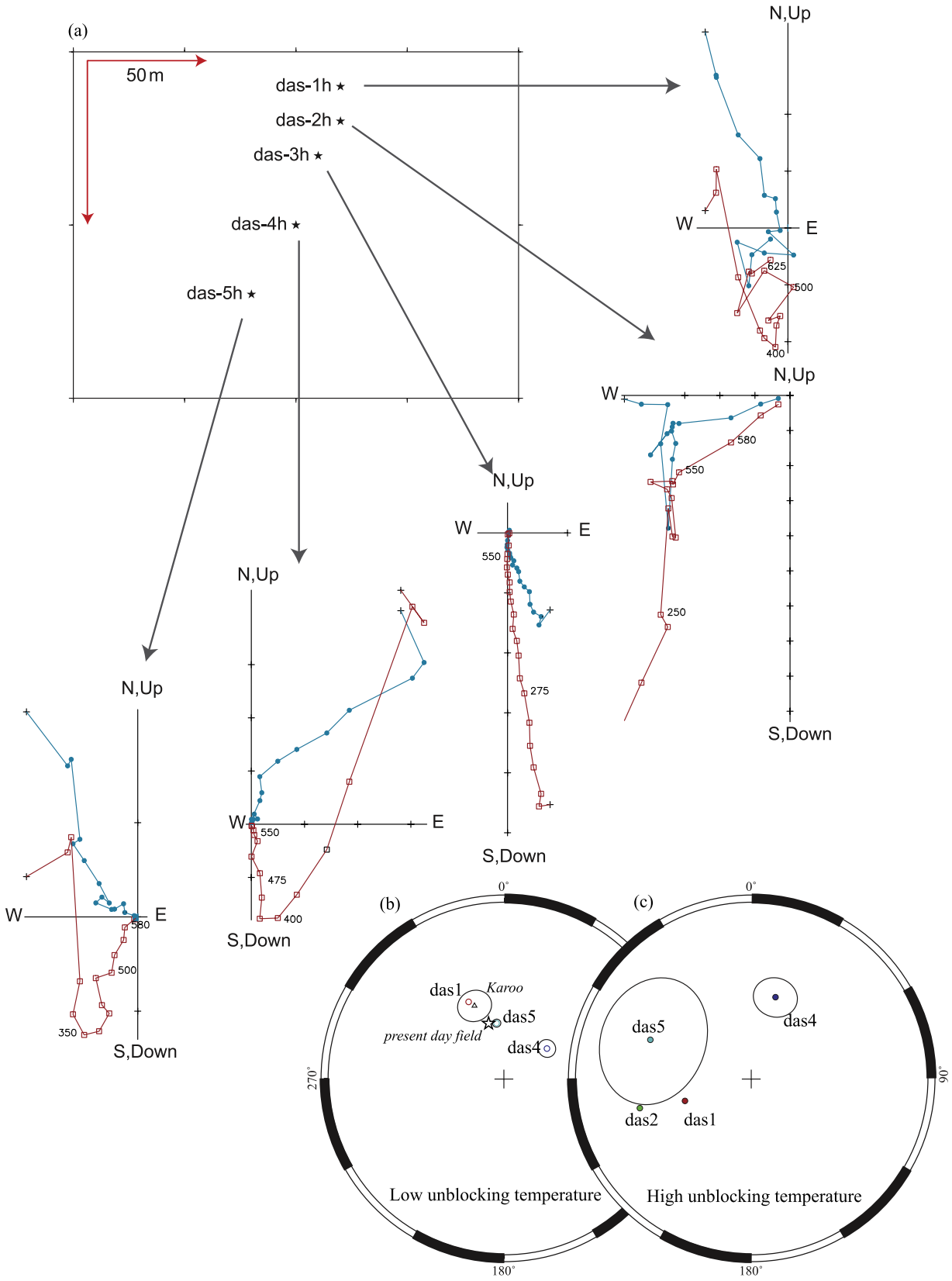
(a)
50 m
das-1h
das-2h
das-3h
das-4h
das-5h
N,Up
W
E
S,Down
625
500
400
580
550
250
275
475
350
(b)
(c)
0°
90°
180°
270°
das1
Karoo
das5
present day field
das4
das2
Low unblocking temperature
High unblocking temperature

Figure 7

Table 3. Low Unblocking Temperature Components From Dacitic Parent Body[a]

Sample	Range (°C)	*N*	MAD	*D* (deg)	*I* (deg)
das1-6	100–425	7	9.2	335.4	−49.8
das4h-0	75–350	8	2.6	46.7	−61.5
das4h-1	200–350	4	2.9	58	−65.5
das4h-2	200–350	4	2.3	58.3	−67.5
das4h-3	200–350	4	2.3	57.8	−66.5
das5h-1	200–400	5	6.9	350	−64.3
das5h-2	200–350	4	3.6	354.7	−63.1
das5h-3	200–350	4	4.5	353.1	−63.4

[a] *N*, number of demagnetization steps used; MAD, maximum angular deviation; *D*, declination; *I*, inclination. Sample naming convention is as follows: example 1, das1-6, locality (das), site (1), and core (6); example 2, das4h-0, locality (das), site (4), hand sample (h), and specimen (0).

or complex multicomponent behavior (see caption, Table 5).

[23] The two-component low and high unblocking temperature nature of the NRM is again seen at site 4, although it appears the high unblocking temperature component may not be completely isolated (i.e., compare orthogonal vector plots from sites 3 and 4 (Figure 7)). The two components appear to be well separated in the hand sample at site 5, but there is scatter within subsamples (Table 4 and Figure 7). Overall, the high unblocking temperature component shows reasonable consistency from sites 1, 2 and 5, whereas the direction from site 4 is quite far removed (Figure 7). Below we discuss interpretations of these data and the related resolution of the conglomerate test.

6. Resolution of the Conglomerate Test: Simple and Exotic Magnetization Scenarios

[24] The magnetic component behavior of the parent dacite as sampled is variable; the presence of single-component magnetizations with highly variable directions is a calling card of terrains hit by modern lightning. The lightning-induced scatter is probably exacerbated by magnetic overprints acquired during low-grade metamorphism (i.e., carried by MD grains).

[25] Although contaminated by modern lightning strikes, results indicate that the parent rocks, like the dacite clasts, contain two dominant components of magnetization: a low unblocking overprint, and a high unblocking temperature component. The low unlocking component is again close to the present-day field and Karoo overprint direction. However, unlike the case of the HT magnetizations from the dacitic conglomerate clasts, the null hypothesis that the high unblocking temperature magnetizations (Table 4, $n = 4$) from the dacite parent body are from a random distribution can be rejected at the 95% confidence level ($R_0 = 3.10$ [*Irving*, 1964]; $R = 3.39$). The simplest interpretation of the HT component is that it records a primary TRM acquired at ~3445 Ma, albeit contaminated by Archean overprints contributing to directional scatter.

[26] While a primary TRM origin is the preferred explanation, we note that the high scatter of the high unblocking temperature component of the parent dacite (spanning some 87° between site 4 and site 1) opens other interpretations. Given the modern and ancient sources of overprinting, and the presence of magnetic grains susceptible to carrying such overprints, we feel it is unwise to attribute this scatter to paleosecular variation (much larger than typical during the last 200 million years). But the data do not necessarily exclude magnetization by a process different from TRM acquisition in a magnetic field generated by core dynamo action. We consider two such scenarios.

[27] The dacite clasts are relatively fresh, but they could have been exposed for a brief time to surface conditions prior to their incorporation into the conglomerate (presumably in water). During this brief surface exposure, they could have been hit by Archean lightning strikes, resulting in a scattered distribution of what we see today as the HT component. This assumes Archean atmospheric conditions conducive to lightning [e.g., *Johnson et al.*, 2008]. Note that this explanation requires all

Figure 7. (a) Map projection (center of projection at latitude −25°56′7.8″, longitude 30°53′42″) of Geluk farm area [see *Lowe and Byerly*, 1999] where the dacite intrusion was sampled with representative orthogonal vector plots of thermal demagnetization shown. Stereonet projections of (b) low unblocking temperature magnetization (Table 3) with the present-day field (star) and Karoo overprint direction (triangle [*Hargraves et al.*, 1997]) (means of subsamples from sites 4 and 5 shown with 95% confidence intervals) and (c) the high unblocking temperature component (Table 4) from sites 1, 2, 4, and 5 (site 3 failed to yield a distinct high unblocking temperature component) (means of subsamples from sites 4 and 5 shown with 95% confidence intervals). All directions are in geographic coordinates.

Table 4. High Unblocking Temperature Components From Dacitic Parent Body[a]

Sample	Range (°C)	N	MAD	D (deg)	I (deg)	k	α_{95}
das1-6	550–580+0	3	12.7	251.8	57.2		
das2-7	550–580+0	3	3.9	255.3	34.3		
das4h-1	550–580+0	3	3.5	16.6	46		
das4h-2	550–580+0	3	8	22.5	55.6		
das4h-3	550–580+0	3	5.4	11.4	46.8		
das4h				*16.5*	*49.5*	*161*	*9.7*
das5h-1	550–580+0	3	3	283.7	37.4		
das5h-2	550–580+0	3	12.3	312	49.8		
das5h-3	550–580+0	3	1.3	283.3	24.5		
das5h				*291.2*	*37.9*	*21*	*27.4*

[a] N, number of demagnetization steps used (does not include the origin); MAD, maximum angular deviation; D, declination; I, inclination; k and α_{95}, *Fisher* [1953] statistical parameters. In the temperature range, "+0" indicates the origin was included in the fit. Sample naming convention is as follows: example 1, das1-6, locality (das), site (1), and core (6); example 2, das4h-1, locality (das), site (4), hand sample (h), and specimen (1). Italics indicate mean values.

clasts listed in Table 2 to have been hit by lightning during the brief surface exposure.

[28] Alternatively, there may have been no dynamo action, as suggested by *Labrosse et al.* [2007], but an external magnetic field may have been present, generated through interaction of the solar wind and the atmosphere. Arguably the best analog for this process in a planet lacking a dynamo is seen in modern-day Venus. Recent exploration of the induced magnetosphere during solar minimum, at periapsis altitudes of 300–250 km, recorded weak fields (by terrestrial standards), ranging from 40 nT to less than 10 nT [*Zhang et al.*, 2007].

[29] Solar wind conditions differed at 3445 Ma [e.g., *Wood*, 2006] and it is conceivable that an induced field on Earth was larger in the distant past. But even if the field were once 2 orders of magnitude greater than that of Venus today, it would still be small relative to Earth's modern field (~50,000 nT) and we would expect it to have a highly time variable character.

[30] Our data do not yield quantitative values on past field strength, and the rocks described here (clasts and parent body site) are too fine-grained for single-crystal analyses with standard high-resolution three-component SQUID systems [*Tarduno et al.*, 2007]. However, other portions of the parent body are coarser grained (and possibly some clasts), and if paleointensity values were available from such samples they could be used to examine these scenarios. In the case of lightning strikes (affecting only clasts as the parent body is intrusive), we would expect to obtain relatively high field values that showed little consistency between samples. In the case of an external field, we would expect extraordinarily low field values (i.e., large TRM capability versus NRM intensity) and large scatter between samples reflecting large fluctuations in external field strength observed at any one site (from diurnal variation to change on longer time scales reflecting solar activity).

[31] We find both of the scenarios outlined above to be unlikely, but strictly speaking the variation of the high unblocking temperature component in the dacite parent body, the presence of multidomain magnetic grains, and the history of low-grade metamorphism introduce ambiguities into interpretation of the data. Below we briefly review other paleomagnetic data reported from Paleoarchean rocks and consider the implications of the simplest interpretation of our data for core evolution.

7. Status of Constraints on Paleoarchean Field Presence/Absence

[32] There have been several prior reports of paleomagnetic and paleointensity data from 3400 to 3500 Ma rocks. Each is now thought to be a record of a later magnetization, although there are often several permissible interpretations of the exact age and mechanism of secondary remanence acquisition. For example, *Hale* [1987] reported paleointensities 4 to 10 times weaker than present-day values from 3500 Ma ultramafic lavas (komatiites) of the Komati Formation. The magnetization is carried by magnetite associated with serpentinite. *Hale and Dunlop* [1984] proposed that the serpentinization occurred soon after eruption of the komatiites, and that the magnetization they hold

Table 5. Samples Showing Single-Component Demagnetization Behavior[a]

Sample	Range (°C)	N	MAD	D (deg)	I (deg)
das1-1	350–580+0	9	15.5	113.7	52
das2-2	325–580+0	13	2.8	125.9	−46.2
das2-3	325–580+0	13	3.8	159.3	−65.9
das2-5	350–580+0	9	7.6	96.9	36.2
das2-6	350–580+0	7	6.1	204	65.4
das3h-0	300–580+0	14	2.9	164.3	71.5

[a] N, number of demagnetization steps used (does not include the origin); MAD, maximum angular deviation; D, declination; I, inclination. In the temperature range, "+0" indicates the origin was included in the fit. Samples that were not fit because of unstable demagnetization behavior included das1-2, das1-7, das2-4, das1h-1, and das1h-2. Sample naming convention is as follows: example 1, das1-1, locality (das), site (1), and core (1); example 2, das3h-0, locality (das), site (3), hand sample (h), and specimen (0).

was a TRM related to intrusion of the nearby Theespruit pluton at ~3.5 Ga. However, in a subsequent study *Yoshihara and Hamano* [2004] concluded that the magnetization was a chemical remanent magnetization related to magnetite grain growth during serpentinization; thus the *Hale* [1987] results cannot be used for standard paleointensity estimation. It is also possible that serpentinization and magnetite formation occurred later, during a tectonothermal event at 3.23 Ga that gave rise to folding and local high-grade metamorphism in the Barberton greenstone belt [*Kamo and Davis*, 1994; *Dziggel et al.*, 2002]. Moreover, *Tarduno et al.* [2007] noted a similarity between the paleomagnetic directions from the komatiites and those of 2782 Ma basalt [*Wingate*, 1998] from South Africa; this similarity together with the suggestion of a regional metamorphic event around that age [*de Ronde et al.*, 1991; *Toulkeridis et al.*, 1998], further suggest it is unlikely that the komatiites retain a ~3500-million-year-old remanence.

[33] *McElhinny and Senanayake* [1980] presented an apparently positive paleomagnetic fold test on pillow basalts and a dacite composite flow of ~3500-million-year age from the Pilbara craton of Australia. Subsequent geochronological investigations have assigned ages of ~3300 to ~3200 Ma for emplacement of a granitoid plutonic complex [*Collins and Gray*, 1990; *Williams and Collins*, 1990] interpreted as the main cause of the folding used for the *McElhinny and Senanayake* [1980] fold test. Moreover, the region has experienced multiple deformation events due to the emplacement of small intrusive units until ~2800 Ma [*Van Kranendonk et al.*, 2002; *Zegers et al.*, 1999]. Fold tests only give ages relative to folding. While the age of folding is uncertain, it is younger than that inferred by *McElhinny and Senanayake* [1980]. Assuming adequate isolation of magnetic components (but see discussion below), the magnetization isolated by these authors could be as young as ~2800 Ma because deformation continued to that time.

[34] There are also problems with the magnetic interpretation in the *McElhinny and Senanayake* [1980] work. The dacite was reported as red in the field, a sign of the severe weathering that has commonly affected the surficial rocks of Western Australia. Yet, *McElhinny and Senanayake* [1980] implied that this color and hematite formation reflected extensive high-temperature oxidation, during initial cooling of the dacite, that was further suggested by the apparent presence of pseudobrookite. This interpretation implies that the highest unblocking temperature component should be the most reliable, as it is this magnetization that should be carried by SD hematite grains. But, the highest unblocking temperature magnetization from the dacite fails the fold test. The positive fold test is based on a lower, intermediate unblocking temperature component from the dacite. Because there is also yet another component of magnetization at still lower unblocking temperatures, it is possible that the intermediate unblocking temperature component identified by *McElhinny and Senanayake* [1980] is an artifact of overlapping secondary magnetizations [*Tarduno et al.*, 2007]. Beyond the uncertainties of the Pilbara dacite magnetizations, it is unclear whether the pillow basalts sampled by *McElhinny and Senanayake* [1980] should be expected to retain a primary magnetization at the unblocking temperatures reported because of the regional upper greenschist metamorphism.

[35] The problems with the *McElhinny and Senanayake* [1980] study have propagated through the literature. In a more recent study of ~3460 Ma chert from the Pilbara craton, *Suganuma et al.* [2006] report directions which they feel are primary in part due to some similarities with those reported by *McElhinny and Senanayake* [1980]. There is no specific evidence that the chert magnetizations are primary, and the rock magnetic data presented indicate the presence of MD grains which would again be expected to carry overprints related to the later metamorphism.

[36] In light of the probably secondary nature of magnetizations reported in prior studies, the data we have presented from the dacite conglomerate and parent rocks (notwithstanding exotic magnetization scenarios) are the most likely to record a primary TRM reflecting a geomagnetic field at ~3445 Ma. The history of the geodynamo is closely related to the evolution of the Earth's interior. The inner core has a significant effect on the geodynamo. Inner core growth provides energy to drive the dynamo through the latent heat of crystallization and the exclusion of light elements [e.g., *Gubbins*, 1977]. The inner core also determines the geometry of outer core flow. Thus, it is possible that the geodynamo operated differently in the absence of an inner core (or, perhaps, it did not operate at all). The possible existence of a magnetic field over the past ~3445 million years, with roughly the present-day strength for at least 3200 million years [*Tarduno et al.*, 2007] is most easily reconciled with an old inner core. Some paleomag-

netic data suggest higher stability of the geomagnetic field during late Archean to early Proterozoic times than at present [*Biggin et al.*, 2008; *Smirnov and Tarduno*, 2004]. This is consistent with a numerical dynamo simulation with a smaller inner core [*Roberts and Glatzmaier*, 2001], but at variance with another simulation without an inner core [*Sakuraba and Kono*, 1999], which produced an unstable geodynamo. These two simulations used different approximations, and the parameter space of both is still greatly different from that of the real Earth. Nevertheless, several recent investigations suggest that a 3500-million-year-old inner core and dynamo are viable [*Buffett*, 2002; *Christensen and Tilgner*, 2004; *Christensen and Aubert*, 2006; *Gubbins et al.*, 2004]. Model calculations of coupled mantle and core thermal evolution that have proposed younger inner core ages of ~2000 to ~1000 Ma [*Labrosse*, 2003; *Labrosse et al.*, 2001; *Nimmo et al.*, 2004] have been criticized for inappropriate core-mantle heat flow [*Davies*, 2007] or geochemically implausible parameterization of the mantle convection [*Korenaga*, 2008; *Lyubetskaya and Korenaga*, 2007], resulting in rapid cooling of the core and/or mantle. Nevertheless, it is clear the origin of the inner core from modeling studies is contentious.

[37] Regardless of the presence or absence of the inner core, secular cooling of the core is essential for the generation of the geodynamo [e.g., *Verhoogen*, 1980]. Absence of the geomagnetic field at 3900 Ma has been proposed on the basis of the abundance and isotopic compositions of nitrogen and noble gases in lunar soil [*Ozima et al.*, 2005]. To generate a dynamo, heat flux from core to mantle must have become high enough to support convection in the liquid iron core. Before the onset of the geodynamo, the core may have been kept from rapid cooling by inefficient plate tectonics [*Korenaga*, 2006, 2008] and/or latent and radiogenic heat from the basal magma ocean [*Labrosse et al.*, 2007]. If a primary TRM recording a geomagnetic field, as is the simplest interpretation, our data suggest that the factors that potentially inhibited dynamo generation had crossed a threshold by 3445 Ma. It is unclear whether conduction through the entire mantle would have been sufficient to drive core convection. Alternatively, establishment of plate tectonics [e.g., *Shirey et al.*, 2008] may have been needed to cool the mantle. These alternatives would result in different core-mantle heat flow evolutions for the earliest geodynamo [*Nimmo and Stevenson*, 2000]. Geomagnetic paleointensity studies, currently underway on the 3445 Ma South African rocks may place more constraints on the energetic state of the ancient core as well as allowing an evaluation of alternative exotic magnetization scenarios.

Acknowledgments

[38] We thank the Mpumalanga Parks Board for access to Songimvelo Nature Reserve. We also thank Pavel Doubrovine for helpful discussions and for providing low-temperature, petrologic, and SEM analyses; Julia Voronov, Allison Sail, and Anna Wendt for assistance in the field; Gerry Kloc for sample preparation; Brian McIntyre for his support in SEM observations; and Toshi Yamazaki for access to the MPMS. We are grateful to David Dunlop, Ted Evans, Josh Feinberg, and an anonymous reviewer for comments on the paper. Y.U. led the laboratory effort on the conglomerate, with assistance from R.C. and J.A.T. R.C. led laboratory study of the source rock with assistance of J.A.T. J.A.T. undertook field studies with M.W. and A.H. This work was supported by the U.S. NSF (to J.A.T.). Y.U. was also supported by JSPS.

References

Armstrong, R. A., W. Compston, W. J. de Wit, and I. S. Williams (1990), The stratigraphy of the 3.5–3.2 Ga Barberton greenstone belt revisited: A zircon ion microprobe study, *Earth Planet. Sci. Lett.*, *101*, 90–106, doi:10.1016/0012-821X(90)90127-J.

Biggin, A. J., G. H. M. A. Strik, and C. G. Langereis (2008), Evidence for a very-long-term trend in geomagnetic secular variation, *Nat. Geosci.*, *1*, 395–398, doi:10.1038/ngeo181.

Buffett, B. A. (2002), Estimates of heat flow in the deep mantle based on the power requirements for the geodynamo, *Geophys. Res. Lett.*, *29*(12), 1566, doi:10.1029/2001GL014649.

Butler, R. F. (1992), *Paleomagnetism: Magnetic Domains to Geologic Terranes*, 319 pp., Blackwell Sci., Boston, Mass.

Byerly, G. R., A. Kroner, D. R. Lowe, W. Todt, and M. M. Walsh (1996), Prolonged magmatism and time constraints for sediment deposition in the early Archean Barberton greenstone belt: Evidence from the Upper Onverwacht and Fig Tree Groups, *Precambrian Res.*, *78*, 125–138, doi:10.1016/0301-9268(95)00073-9.

Cathelineau, M. (1988), Cation site occupancy in chlorites and illites as a function of temperature, *Clay Miner.*, *23*, 471–485, doi:10.1180/claymin.1988.023.4.13.

Christensen, U. R., and J. Aubert (2006), Scaling properties of convection-driven dynamos in rotating spherical shells and application to planetary magnetic field, *Geophys. J. Int.*, *166*, 97–114, doi:10.1111/j.1365-246X.2006.03009.x.

Christensen, U. R., and A. Tilgner (2004), Power requirement of the geodynamo from ohmic losses in numerical and laboratory dynamos, *Nature*, *429*, 169–171, doi:10.1038/nature02508.

Cloete, M. (1999), *Aspects of Volcanism and Metamorphism of the Onverwacht Group Lavas in the Southwestern Portion of the Barberton Greenstone Belt*, *Mem. Geol. Surv. S. Afr.*, *84*, 232 pp.

Collins, W. J., and C. M. Gray (1990), Rb-Sr isotopic systematics of an Archean granite-gneiss terrain: The Mount Edgar Batholith, Pilbara Block, Western Australia, *Aust. J. Earth Sci.*, *37*, 9–22, doi:10.1080/08120099008727901.

Cottrell, R. D., and J. A. Tarduno (1999), Geomagnetic paleointensity derived from single plagioclase crystals, *Earth Planet. Sci. Lett.*, *169*, 1–5, doi:10.1016/S0012-821X(99)00068-0.

Davies, G. (2007), Mantle regulation of core cooling: A geodynamo without core radioactivity?, *Phys. Earth Planet. Inter.*, *160*, 215–229, doi:10.1016/j.pepi.2006.11.001.

Day, R., M. D. Fuller, and V. A. Schmidt (1977), Hysteresis properties of titanomagnetites: Grain size and composition dependence, *Phys. Earth Planet. Inter.*, *13*, 260–267, doi:10.1016/0031-9201(77)90108-X.

de Ronde, C. E. J., C. M. Hall, D. York, and E. T. C. Spooner (1991), Laser step-heating $^{40}Ar/^{39}Ar$ age spectra from Early Archean (~3.5 Ga) Barberton greenstone belt sediments: A technique for detecting cryptic tectono-thermal events, *Geochim. Cosmochim. Acta*, *55*, 1933–1951, doi:10.1016/0016-7037(91)90034-3.

de Vries, S. T., W. Nijman, and R. A. Armstrong (2006), Growth-fault structure and stratigraphic architecture of the Buck Ridge volcano-sedimentary complex, upper Hooggenoeg Formation, Barberton Greenstone Belt, South Africa, *Precambrian Res.*, *149*, 77–98, doi:10.1016/j.precamres.2006.04.005.

de Wit, M. J., R. Armstrong, R. J. Hatt, and A. H. Wilson (1987), Felsic igneous rocks within the 3.3–3.5-Ga Barberton greenstone belt: High crustal level equivalents of the surrounding tonalite-trondhremite terrain, emplaced during thrusting, *Tectonics*, *6*, 529–549, doi:10.1029/TC006i005p00529.

Dunlop, D. J. (2002), Theory and application of the Day plot (M_{rs}/M_s versus H_{cr}/H_c): 1. Theoretical curves and tests using titanomagnetite data, *J. Geophys. Res.*, *107*(B3), 2056, doi:10.1029/2001JB000486.

Dunlop, D. J., and Ö. Özdemir (1997), *Rock Magnetism: Fundamentals and Frontiers*, 596 pp., Cambridge Univ. Press, Cambridge, U. K.

Dziggel, A., G. Stevens, M. Poujol, C. R. Anhaeusset, and R. A. Armstrong (2002), Metamorphism of the granite-greenstone terrane south of the Barberton greenstone belt, South Africa: An insight into the tectono-thermal evolution of the lower portions of the Onverwacht Group, *Precambrian Res.*, *114*, 221–247, doi:10.1016/S0301-9268(01)00225-X.

Fisher, R. A. (1953), Dispersion on a sphere, *Proc. R. Soc. London, Ser. A*, *217*, 295–305, doi:10.1098/rspa.1953.0064.

Graham, J. W. (1949), The stability and significance of magnetism in sedimentary rock, *J. Geophys. Res.*, *54*, 131–167, doi:10.1029/JZ054i002p00131.

Gubbins, D. (1977), Energetics of the Earth's core, *J. Geophys.*, *43*, 453–464.

Gubbins, D., D. Alfe, G. Masters, G. D. Price, and M. Gillan (2004), Gross thermodynamics of two-component core convection, *Geophys. J. Int.*, *157*, 1407–1414, doi:10.1111/j.1365-246X.2004.02219.x.

Hale, C. J. (1987), The intensity of the geomagnetic field at 3.5 Ga: Paleointensity results from the Komati Formation, Barberton Mountain Land, South Africa, *Earth Planet. Sci. Lett.*, *86*, 354–364, doi:10.1016/0012-821X(87)90232-9.

Hale, C. J., and D. J. Dunlop (1984), Evidence for an Early Archean geomagnetic field: A paleomagnetic study of the Komati Formation, Barberton Greenstone Belt, South Africa, *Geophys. Res. Lett.*, *11*, 97–100, doi:10.1029/GL011i002p00097.

Hargraves, R. B., J. Rehacek, and P. R. Hooper (1997), Palaeomagnetism of the Karoo igneous rocks in southern Africa, *S. Afr. J. Geol.*, *100*(2), 195–212.

Irving, E. (1964), *Paleomagnetism and Its Application to Geological and Geophysical Problems*, 399 pp., John Wiley, New York.

Jackson, M., P. Rochette, G. Fillion, S. K. Banerjee, and J. Marvin (1993), Rock magnetism of remagnetized Paleozoic carbonates: Low-temperature behavior and susceptibility characteristics, *J. Geophys. Res.*, *98*, 6217–6225, doi:10.1029/92JB01319.

Johnson, A. P., H. J. Cleaves, J. P. Dworkin, D. P. Glavin, A. Lazcano, and J. L. Bada (2008), The Miller volcanic spark discharge experiment, *Science*, *322*, 404, doi:10.1126/science.1161527.

Johnson, H. P., and J. M. Hall (1978), A detailed rock magnetic and opaque mineralogy study of the basalts from the Nazca Plate, *Geophys. J. R. Astron. Soc.*, *52*, 45–64.

Kamo, S. L., and D. W. Davis (1994), Reassessment of Archean crustal development in the Barberton Mountain Land, South Africa, based on U-Pb dating, *Tectonics*, *13*, 167–192, doi:10.1029/93TC02254.

Kirschvink, J. L. (1980), The least-squares line and plane and the analysis of paleomagnetic data, *Geophys. J. R. Astron. Soc.*, *62*, 699–718.

Kirschvink, J. L., A. T. Maine, and H. Vali (1997), Paleomagnetic evidence of a low-temperature origin of carbonate in the Martian meteorite ALH8401, *Science*, *275*(5306), 1629–1633, doi:10.1126/science.275.5306.1629.

Korenaga, J. (2006), Archean geodynamics and the thermal evolution of Earth, in *Archean Geodynamics and Environments*, *Geophys. Monogr. Ser.*, vol. 164, edited by K. Benn, J.-C. Mareschal, and K. Condie, pp. 7–32AGU, Washington, D. C.

Korenaga, J. (2008), Urey ratio and the structure and evolution of Earth's mantle, *Rev. Geophys.*, *46*, RG2007, doi:10.1029/2007RG000241.

Kröner, A., and W. Todt (1988), Single zircon dating constraining the maximum age of the Barberton greenstone belt, South Africa, *J. Geophys. Res.*, *93*, 15,329–15,337, doi:10.1029/JB093iB12p15329.

Kröner, A., G. R. Byerly, and D. R. Lowe (1991), Chronology of early Archean granite-greenstone evolution in the Barberton Mountain land, South Africa, based on precise dating by single zircon evaporation, *Earth Planet. Sci. Lett.*, *103*, 41–45, doi:10.1016/0012-821X(91)90148-B.

Labrosse, S. (2003), Thermal and magnetic evolution of the Earth's core, *Phys. Earth Planet. Inter.*, *140*, 127–143, doi:10.1016/j.pepi.2003.07.006.

Labrosse, S., J.-P. Poirier, and J.-L. Le Mouël (2001), The age of the inner core, *Earth Planet. Sci. Lett.*, *190*, 111–123, doi:10.1016/S0012-821X(01)00387-9.

Labrosse, S., J. W. Hernlund, and N. Coltice (2007), A crystallizing dense magma ocean at the base of the Earth's mantle, *Nature*, *450*, 866–869, doi:10.1038/nature06355.

Lowe, D. R., and G. R. Byerly (1999), Stratigraphy of the west-central part of the Barberton Greenstone Belt, South Africa, in *Geologic Evolution of the Barberton Greenstone Belt, South Africa*, edited by D. R. Lowe and G. R. Byerly, *Spec. Pap. Geol. Soc. Am.*, *329*, 1–36.

Lyubetskaya, T., and J. Korenaga (2007), Chemical composition of Earth's primitive mantle and its variance: 2. Implications for global geodynamics, *J. Geophys. Res.*, *112*, B03212, doi:10.1029/2005JB004224.

McElhinny, M. W. (1973), *Palaeomagnetism and Plate Tectonics*, 358 pp., Cambridge Univ. Press, Cambridge, U. K.

McElhinny, M. W., and W. E. Senanayake (1980), Paleomagnetic evidence for the existence of the geomagnetic field at

3.5 Ga ago, *J. Geophys. Res.*, *85*, 3523–3528, doi:10.1029/JB085iB07p03523.

Néel, L. (1955), Some theoretical aspects of rock magnetism, *Adv. Phys.*, *4*, 191–243, doi:10.1080/00018735500101204.

Nimmo, F., and D. J. Stevenson (2000), The influence of plate tectonics on the thermal evolution and magnetic field of Mars, *J. Geophys. Res.*, *105*, 11,969–11,980, doi:10.1029/1999JE001216.

Nimmo, F., G. D. Price, J. Brodholt, and D. Gubbins (2004), The influence of potassium on core and geodynamo evolution, *Geophys. J. Int.*, *156*, 363–376, doi:10.1111/j.1365-246X.2003.02157.x.

O'Reilly, W., and S. K. Banerjee (1967), The mechanism of oxidation in titanomagnetites: A magnetic study, *Min. Mag.*, *36*, 29–37, doi:10.1180/minmag.1967.036.277.04.

Özdemir, Ö., D. J. Dunlop, and B. M. Moskowitz (1993), The effect of oxidation on the Verwey transition in magnetite, *Geophys. Res. Lett.*, *20*, 1671–1674, doi:10.1029/93GL01483.

Ozima, M., K. Seki, N. Terada, Y. N. Miura, F. A. Podosek, and H. Shinagawa (2005), Terrestrial nitrogen and noble gases in lunar soils, *Nature*, *436*, 655–659, doi:10.1038/nature03929.

Petersen, N., and H. Vali (1987), Observation of shrinkage cracks in ocean floor titanomagnetites, *Phys. Earth Planet. Inter.*, *46*, 197–205, doi:10.1016/0031-9201(87)90182-8.

Roberts, P. H., and G. A. Glatzmaier (2001), The geodynamo, past, present and future, *Geophys. Astrophys. Fluid Dyn.*, *94*, 47–84, doi:10.1080/03091920108204131.

Sakuraba, A., and M. Kono (1999), Effect of the inner core on the numerical solution of the magnetohydrodynamic dynamo, *Phys. Earth Planet. Inter.*, *111*, 105–121, doi:10.1016/S0031-9201(98)00150-2.

Shirey, S. B., B. S. Kamber, M. J. Whitehouse, P. A. Mueller, and A. R. Basu (2008), A review of the isotopic and trace element evidence for mantle and crustal processes in the Hadean and Archean: Implication for the onset of plate tectonic subduction, in *When Did Plate Tectonics Begin on Planet Earth?*, edited by K. C. Condie and V. Pease, *Spec. Pap. Geol. Soc. Am.*, *440*, 1–29.

Smirnov, A. V., and J. A. Tarduno (2004), Secular variation of the Late Archean–Early Proterozoic geodynamo, *Geophys. Res. Lett.*, *31*, L16607, doi:10.1029/2004GL020333.

Smirnov, A. V., J. A. Tarduno, and B. N. Pisakin (2003), Paleointensity of the early geodynamo (2.45 Ga) as recorded in Karelia: A single crystal approach, *Geology*, *31*, 415–418, doi:10.1130/0091-7613(2003)031<0415:POTEGG>2.0.CO;2.

South African Committee for Stratigraphy (1980), *Stratigraphy of South Africa*, *Handb. S. Afr. Geol. Surv.*, *8*(1), 690 pp.

Strik, G., M. J. de Wit, and C. G. Langereis (2007), Palaeomagnetism of the Neoarchaean Pongola and Ventersdorp Supergroups and an appraisal of the 3.0–1.9 Ga apparent polar wonder path of the Kaapvaal Craton, southern Africa, *Precambrian Res.*, *153*, 96–115, doi:10.1016/j.precamres.2006.11.006.

Suganuma, Y., Y. Hamano, S. Niitsuma, M. Hoashi, T. Hisamitsu, N. Niitsuma, K. Kodama, and M. Nedachi (2006), Paleomagnetism of the Marble Bar Chert Member, Western Australia: Implication for apparent polar wander path for Pilbara craton during Archean time, *Earth Planet. Sci. Lett.*, *252*, 360–371, doi:10.1016/j.epsl.2006.10.003.

Tarduno, J. A., and M. Myers (1994), A primary magnetization fingerprint from the Cretaceous Laytonville Limestone: Further evidence for rapid oceanic plate velocities, *J. Geophys. Res.*, *99*, 21,691–21,703, doi:10.1029/94JB01939.

Tarduno, J. A., R. D. Cottrell, and A. V. Smirnov (2006), The paleomagnetism of single silicate crystals: Recording geomagnetic field strength during mixed polarity intervals, superchrons and inner core growth, *Rev. Geophys.*, *44*, RG1002, doi:10.1029/2005RG000189.

Tarduno, J. A., R. D. Cottrell, M. K. Watkeys, and D. Bauch (2007), Geomagnetic field strength 3.2 billion years ago recorded by single silicate crystals, *Nature*, *446*, 657–660, doi:10.1038/nature05667.

Tauxe, L., T. A. T. Mullender, and T. Pick (1996), Potbellies, wasp-waists, and superparamagnetism in magnetic Hysteresis, *J. Geophys. Res.*, *101*, 571–583, doi:10.1029/95JB03041.

Tice, M. M., B. C. Bostick, and D. R. Lowe (2004), Thermal history of the 3.5–3.2 Ga Onverwacht and Fig Tree Groups, Barberton greenstone belt, South Africa, inferred by Raman microspectroscopy of carbonaceous material, *Geology*, *32*, 37–40, doi:10.1130/G19915.1.

Toulkeridis, T., S. L. Goldstein, N. Clauer, A. Kröner, W. Todt, and M. Schidlowski (1998), Sm-Nd, Rb-Sr and Pb-Pb dating of silicic carbonates from the Early Archean Barberton greenstone belt, South Africa: Evidence for postdepositional isotopic resetting at low temperature, *Precambrian Res.*, *92*, 129–144, doi:10.1016/S0301-9268(98)00071-0.

Van Kranendonk, M. J., A. H. Hickman, R. H. Smithies, D. R. Nelson, and G. Pike (2002), Geology and tectonic evolution of the Archean North Pilbara Terrain, Pilbara Craton, Western Australia, *Econ. Geol.*, *97*, 695–732, doi:10.2113/97.4.695.

Verhoogen, J. (1980), *Energetics of the Earth*, 139 pp., Natl. Acad. of Sci., Washington, D. C.

Verwey, E. J. W. (1939), Electronic conduction of magnetite (Fe_3O_4) and its transition point at low-temperature, *Nature*, *144*, 327–328, doi:10.1038/144327b0.

Viljoen, R. P., and M. J. Viljoen (1969), An introduction to the geology of the Barberton granite-greenstone terrain, *Spec. Publ. Geol. Soc. S. Afr.*, *9*, 1–20.

Watson, G. S. (1956), A test for randomness of directions, *Geophys. J. Int.*, *7*(S4), 160–161, doi:10.1111/j.1365-246X.1956.tb05561.x.

Weiss, B. P., H. Vali, F. J. Baudenbacher, J. L. Kirschvink, S. T. Stewart, and D. L. Shuster (2002), Records of an ancient Martian magnetic field in ALH84001, *Earth Planet. Sci. Lett.*, *201*, 449–463, doi:10.1016/S0012-821X(02)00728-8.

Williams, I. S., and W. J. Collins (1990), Granite-greenstone terranes in the Pilbara Block, Australia, as coeval volcano-plutonic complexes; Evidence from U-Pb zircon dating of the Mount Edgar Batholith, *Earth Planet. Sci. Lett.*, *97*, 41–53, doi:10.1016/0012-821X(90)90097-H.

Wingate, M. T. D. (1998), A paleomagnetic test of the Kaapvaal–Pilbara (Vaalbara) connection at 2.78 Ga, *S. Afr. J. Geol.*, *101*(4), 257–274.

Wood, B. E. (2006), The solar wind and the sun in the past, *Space Sci. Rev.*, *126*, 3–14, doi:10.1007/s11214-006-9006-0.

Xie, X., G. R. Byerly, and R. E. Ferrell (1997), IIb trioctahedral chlorite from the Barberton greenstone belt: Crystal structure and rock composition constraints with implications to geothermometry, *Contrib. Mineral. Petrol.*, *126*, 275–291, doi:10.1007/s004100050250.

Yoshihara, A., and Y. Hamano (2004), Paleomagnetic constraints on the Archean geomagnetic field intensity obtained from komatiites of the Barberton and Belingwe greenstone

belts, South Africa and Zimbabwe, *Precambrian Res.*, *131*, 111–142, doi:10.1016/j.precamres.2004.01.003.

Zegers, T. E., J. R. Wijbrans, and S. H. White (1999), $^{40}Ar/^{39}Ar$ age constraints on tectonothermal events in the Shaw area of the eastern Pilbara granite-greenstone terrain (W Australia): 700 Ma of Archean tectonic evolution, *Tectonophysics*, *311*, 45–81, doi:10.1016/S0040-1951(99)00157-2.

Zhang, T. L., et al. (2007), Little or no solar wind enters Venus' atmosphere at solar minimum, *Nature*, *450*, 654–656, doi:10.1038/nature06026.